Foxn4 is a temporal identity factor conferring mid/late-early retinal competence and involved in retinal synaptogenesis

Shuting Liu[a,1], Xiaoning Liu[a,1], Shengguo Li[b,c], Xiuting Huang[a], Haohua Qian[d], Kangxin Jin[a,2], and Mengqing Xiang[a,2]

[a]State Key Laboratory of Ophthalmology, Zhongshan Ophthalmic Center, Sun Yat-sen University, 510060 Guangzhou, China; [b]Center for Advanced Biotechnology and Medicine, Rutgers Robert Wood Johnson Medical School, Piscataway, NJ 08854; [c]Department of Pediatrics, Rutgers Robert Wood Johnson Medical School, Piscataway, NJ 08854; and [d]Visual Function Core, National Eye Institute, National Institutes of Health, Bethesda, MD 20892

Edited by Jeremy Nathans, Johns Hopkins University School of Medicine, Baltimore, MD, and approved January 24, 2020 (received for review October 24, 2019)

During development, neural progenitors change their competence states over time to sequentially generate different types of neurons and glia. Several cascades of temporal transcription factors (tTFs) have been discovered in *Drosophila* to control the temporal identity of neuroblasts, but the temporal regulation mechanism is poorly understood in vertebrates. Mammalian retinal progenitor cells (RPCs) give rise to several types of neuronal and glial cells following a sequential yet overlapping temporal order. Here, by temporal cluster analysis, RNA-sequencing analysis, and loss-of-function and gain-of-function studies, we show that the Fox domain TF Foxn4 functions as a tTF during retinogenesis to confer RPCs with the competence to generate the mid/late-early cell types: amacrine, horizontal, cone, and rod cells, while suppressing the competence of generating the immediate-early cell type: retinal ganglion cells (RGCs). In early embryonic retinas, *Foxn4* inactivation causes down-regulation of photoreceptor marker genes and decreased photoreceptor generation but increased RGC production, whereas its overexpression has the opposite effect. Just as in *Drosophila*, Foxn4 appears to positively regulate its downstream tTF Casz1 while negatively regulating its upstream tTF Ikzf1. Moreover, retina-specific ablation of *Foxn4* reveals that it may be indirectly involved in the synaptogenesis, establishment of laminar structure, visual signal transmission, and long-term maintenance of the retina. Together, our data provide evidence that Foxn4 acts as a tTF to bias RPCs toward the mid/late-early cell fates and identify a missing member of the tTF cascade that controls RPC temporal identities to ensure the generation of proper neuronal diversity in the retina.

Foxn4 | temporal transcription factor | retinal progenitor | photoreceptor | synaptogenesis

The mammalian retina is composed of 6 major neuronal cell types, namely rod, cone, horizontal, bipolar, amacrine, and retinal ganglion cells (RGCs), and 1 type of glia, the Müller cells. During retinogenesis, multipotent retinal progenitor cells (RPCs) give birth to all of the 7 cell types following a sequential yet overlapping temporal order (1–3). As retinogenesis progresses from embryonic to postnatal stages, the progenitors are thought to progressively change their competence states for the ordered generation of the 7 retinal cell types (4–6). Thus, early embryonic RPCs are competent to generate only RGCs and amacrine, horizontal, and photoreceptor cells, whereas late postnatal RPCs can generate only rod, bipolar, and Müller cells. At present, it is unclear how these temporal competence states are established in RPCs (7).

In *Drosophila*, several cascades of temporal transcription factors (tTFs) have been found to control temporal identities of neuroblasts for the sequential generation of stereotyped neurons and glia (8–10). In mice, the Ikzf1 zinc finger TF was identified as the ortholog of *Drosophila* Hunchback, one of the neuroblast tTFs in the temporal cascade governing sequential generation of diverse lineages in the embryonic ventral nerve cord (VNC) (11, 12). Ikzf1 is involved in defining the early competence states of RPCs responsible for generating early-born cell types including early-born RGCs and amacrine and horizontal cells (12). The Casz1 zinc finger TF is a homolog of another *Drosophila* tTF, Castor, in the VNC cascade. It makes rodent RPCs competent for the generation of mid/late-born cell types including rod and bipolar cells (13). The identification of Ikzf1 and Casz1 suggests that the temporal identity of mammalian RPCs may be conferred also by a cascade of tTFs similar to those operating in *Drosophila* neuroblasts. However, this putative cascade appears to be far from complete. For instance, Ikzf1 and Casz1 are not involved in the generation of the early-born cell type, cones, or the late-born cell type, Müller cells (8). Given the time windows represented by these 2 missing cell types, by inference, at least 2 tTFs but likely more remain to be identified.

Previously, we and others have shown that the Fox domain TF Foxn4 is crucial to the development of retina (14–19), spinal cord (20–23), and alveoli (24) in mammals, heart (25) in zebrafish, and skin in *Xenopus* (26). During retinal development, Foxn4 coordinates with the retinoid-related orphan nuclear receptor β1 (RORβ1) (14, 27), and together up-regulates expression of downstream genes such as *Ptf1a* (28, 29). This TF and signaling

Significance

Organogenesis, an evolutionarily refined process which is so complicated, delicate, yet replicable, is all about time and space. Only until recently have scientists realized that the temporal identity of *Drosophila* neuroblasts is controlled by cascades of temporal transcription factors (tTFs), but the temporal regulation mechanism is poorly understood in vertebrates. We show that Foxn4 functions as a tTF to confer mammalian retinal progenitors (RPCs) with the competence to generate mid/late-early cell types while suppressing the immediate-early cell type. Our data thus identify a missing member of the tTF cascade that controls RPC temporal identities to ensure the generation of proper retinal neuronal diversity, and provide an important insight for understanding how cell-fate transitions are guided during vertebrate organogenesis.

Author contributions: K.J. and M.X. designed research; S. Liu, X.L., S. Li, X.H., H.Q., K.J., and M.X. performed research; S. Liu, X.L., S. Li, H.Q., K.J., and M.X. analyzed data; and K.J. and M.X. wrote the paper.

The authors declare no competing interest.

This article is a PNAS Direct Submission.

[1]S. Liu and X.L. contributed equally to this work.

[2]To whom correspondence may be addressed. Email: jinkx@mail.sysu.edu.cn or xiangmq3@mail.sysu.edu.cn.

This article contains supporting information online at https://www.pnas.org/lookup/suppl/doi:10.1073/pnas.1918628117/-/DCSupplemental.

First published February 18, 2020.

cascade leads to the specification and differentiation of amacrine and horizontal cells. Concomitantly, Foxn4 directly activates the transcription of *Dll4*, which encodes a delta-like ligand that binds to Notch receptors on neighboring progenitors and inhibits their differentiation toward photoreceptors (17). Indeed, as a result of *Foxn4* knockout, there was a temporary increase of the photoreceptor population during development (14).

To further understand the regulatory function of Foxn4 during retinal development, we performed a temporal cluster analysis of Foxn4-dependent genes at different developmental stages and generated retina-specific conditional *Foxn4*-knockout mice. Through these functional rather than homology screening studies, our data revealed that Foxn4 may act as a tTF during retinogenesis to confer RPCs with the competence to generate cone, rod, amacrine, and horizontal cells, and that it may be indirectly required for the synaptogenesis and long-term maintenance of the adult retina.

Results

Abnormal Temporal Changes of Photoreceptor Gene Expression in *Foxn4*-Null Retinas Revealed by Microarray and RNA-Seq Analyses. Previously, we identified by microarray analysis differentially expressed genes in embryonic day (E)14.5 $Foxn4^{lacZ/lacZ}$ retinas (14, 17). To further understand the molecular basis of retinal phenotypes in $Foxn4^{lacZ/lacZ}$ animals, we carried out microarray analysis of later-stage retinas using Affymetrix Mouse Genome 430A arrays. Array hybridization was carried out in quadruplicate using probes derived from E16.5 and postnatal day (P)0 retinas of $Foxn4^{+/+}$ and $Foxn4^{lacZ/lacZ}$ animals (14). The obtained data were then analyzed using Microarray Suite and dChip software (30) to calculate fold changes of transcripts between the control and mutant. We identified 554 unique transcripts that displayed ≥1.7-fold change (decrease or increase) in their expression levels in *Foxn4*-null retinas for at least one of the three developmental stages (E14.5, E16.5, and P0). These transcripts were analyzed by Genesis software (31) to reveal 4 hierarchical clusters, A to D (Fig. 1 *A*–*E*).

Among the 4 clusters, cluster C is the largest, representing genes whose expression is down-regulated in the mutant retina at E14.5, E16.5, and P0 (Fig. 1 *A* and *D*). Consistent with the known functions of Foxn4 in specifying the amacrine and horizontal cell fates (14), included in cluster C are *Ptf1a*, *Tfap2a*, *Tfap2b*, *Prox1*, and *Lhx9*, which are TF genes involved in the specification and differentiation of amacrine and horizontal cells (Dataset S1). Cluster B represents genes whose expression is initially down-regulated at E14.5 but gradually up-regulated from E16.5 to P0 (Fig. 1 *A* and *C*). Unexpectedly, enriched in cluster B are many photoreceptor genes (Fig. 1*F*). These include TF genes *Otx2*, *Crx*, *Nrl*, *Prdm1*, and *Rxrg* (7, 32) (Fig. 1*F*), which are required for photoreceptor cell specification and differentiation, as well as a number of photoreceptor-specific genes including *Pdc*, *Gnat2*, *Gnb3*, and *Abca4* (Fig. 1*F*). Although the up-regulation of the photoreceptor genes in P0 $Foxn4^{lacZ/lacZ}$ retinas is consistent with increased photoreceptor cells observed in *Foxn4*-null retinas at postnatal stages (14), their down-regulation in E14.5 null retinas suggests a possibility that Foxn4 may be required for photoreceptor generation instead of suppressing it at early embryonic stages.

To further confirm down-regulation of photoreceptor genes in E14.5 $Foxn4^{lacZ/lacZ}$ retinas, we carried out RNA-seq (sequencing) analysis to identify genes differentially expressed in the mutant retina. This analysis identified 949 genes whose expression level changed (down-regulated or up-regulated) by more than 1.5-fold in the null retina (Fig. 1*G*, *SI Appendix*, Fig. S1 *A* and *B*, and Dataset S2). We performed gene set enrichment analysis of these differentially expressed genes followed by network visualization, which revealed a clustered network of gene ontology terms for a set of down-regulated genes (*SI Appendix*, Fig. S1*C*). These genes are enriched for those involved in neural development such as CNS development, brain development, sensory organ development, cell-fate commitment, neuron differentiation, pattern specification process, and regionalization (*SI Appendix*, Fig. S1*C*). In agreement with the microarray data which have ∼30% gene overlap with the RNA-seq data, the down-regulated genes include a set of photoreceptor genes, for example, *Otx2*, *Crx*, *Prdm1*, *Onecut1*, and so forth (Fig. 1*H*), implicating a photoreceptor generation defect in E14.5 $Foxn4^{lacZ/lacZ}$ retinas.

Validation of Temporal Changes of Photoreceptor Gene Expression in *Foxn4*-Null Retinas. To validate the aberrant temporal changes of photoreceptor gene expression in *Foxn4* mutant retinas, we performed RNA in situ hybridization for *Otx2*, *Prdm1*, *Crx*, and *Thrb*. Indeed, these photoreceptor TF genes exhibited a dynamic temporal expression pattern characteristic of cluster B in the mutant retina. At E14.5, E16.5, and P0, their signals were primarily located at the outer edge of control retinas, where newborn photoreceptor cells reside (Fig. 2 *A*–*X*). In $Foxn4^{lacZ/lacZ}$ retinas, there were barely any *Otx2*, *Prdm1*, *Crx*, and *Thrb* signals detected at E14.5 at the outer edge, but their signals recovered to various but substantial levels at E16.5 and by P0 became obviously stronger than those in control retinas (Fig. 2 *A*–*X*). These dynamic temporal patterns are consistent with the anomalous temporal patterns of photoreceptor gene expression revealed by cluster analysis in mutant retinas. In agreement with the cluster and in situ hybridization analyses, in $Foxn4^{lacZ/lacZ}$ retinas, qRT-PCR assay also showed a significant decrease in the expression levels of photoreceptor genes *Crx*, *Nrl*, *Nr2e3*, *Gnat1*, *Pdc*, and *Rom1* at E14.5 but a significant increase in their expression levels at P0 (Fig. 2*Y*). Their expression recovered to various levels by E16.5, with some reaching wild-type levels or even more (Fig. 2*Y*).

The fact that *Foxn4* inactivation leads to alteration of photoreceptor gene expression suggests that Foxn4 may directly and/or indirectly regulate photoreceptor gene expression in retinal progenitors. We therefore investigated whether Foxn4 is colocalized with photoreceptor transcriptional regulatory genes in progenitors. The single-cell RNA-seq (scRNA-seq) data of murine retinal cells from stages E11 to P14 (33) were analyzed for gene coexpression patterns. We found that *Foxn4* was colocalized extensively with *Otx2* and partially with *Prdm1* in a subpopulation of single RPCs, whereas it essentially had no colocalization with *Crx*, *Nrl*, *Nr2e3*, *Thrb*, *Rxrg*, and *Onecut1* (Fig. 2*Z*). Stage-specific analysis revealed similar colocalization between *Foxn4* and *Otx2* at E11, E12, E14, and E18 (*SI Appendix*, Fig. S2). Furthermore, immunostaining showed that in E13.5 mouse retinas, ∼30 to 40% of $Foxn4^{+}$ or $Otx2^{+}$ cells were double-positive for both Foxn4 and Otx2 (Fig. 2 *A′* and *B′*), suggesting that Foxn4 may be able to activate *Otx2* expression in the same RPCs.

Impaired Photoreceptor Generation in Early Embryonic *Foxn4*-Null Retinas. Given the down-regulation of photoreceptor genes in *Foxn4*-null retinas at E14.5, we asked whether there was a defect in photoreceptor generation in the mutant at early embryonic stages. In E15.5 $Foxn4^{lacZ/lacZ}$ retinas, compared with the control, most Rxrg-immunoreactive cones located at the outer edge were missing (Fig. 3 *A* and *B*), indicating a defect of cone cell generation. To more directly assess photoreceptor generation during early retinogenesis, we labeled newborn cells with bromodeoxyuridine (BrdU) at E12.5 and then collected labeled retinas at P0 for double-immunostaining analysis with anti-recoverin and anti-BrdU antibodies. We found that the proportion of $recoverin^{+}$ photoreceptor cells colabeled by BrdU was reduced by more than 2-fold in $Foxn4^{lacZ/lacZ}$ retinas compared with the control (Fig. 3 *C*–*F*). Thus, during early retinogenesis, Foxn4 appears to positively control the expression of photoreceptor genes and its inactivation leads to diminished photoreceptor generation.

Promotion of Photoreceptor Generation in Early Embryonic Retinas by Foxn4. Given the requirement of Foxn4 in generating photoreceptors in early embryonic retinas, we investigated its sufficiency to promote their generation at early stages. We overexpressed Foxn4 by electroporating ex vivo pCIG-Foxn4 and pCIG plasmid DNA (17) (Fig. 3*G*) into E13.5 mouse retinas. Following a 3-day (d) culture of the electroporated retinas, we found that misexpressed Foxn4 increased $Rxrg^{+}$ cones (located

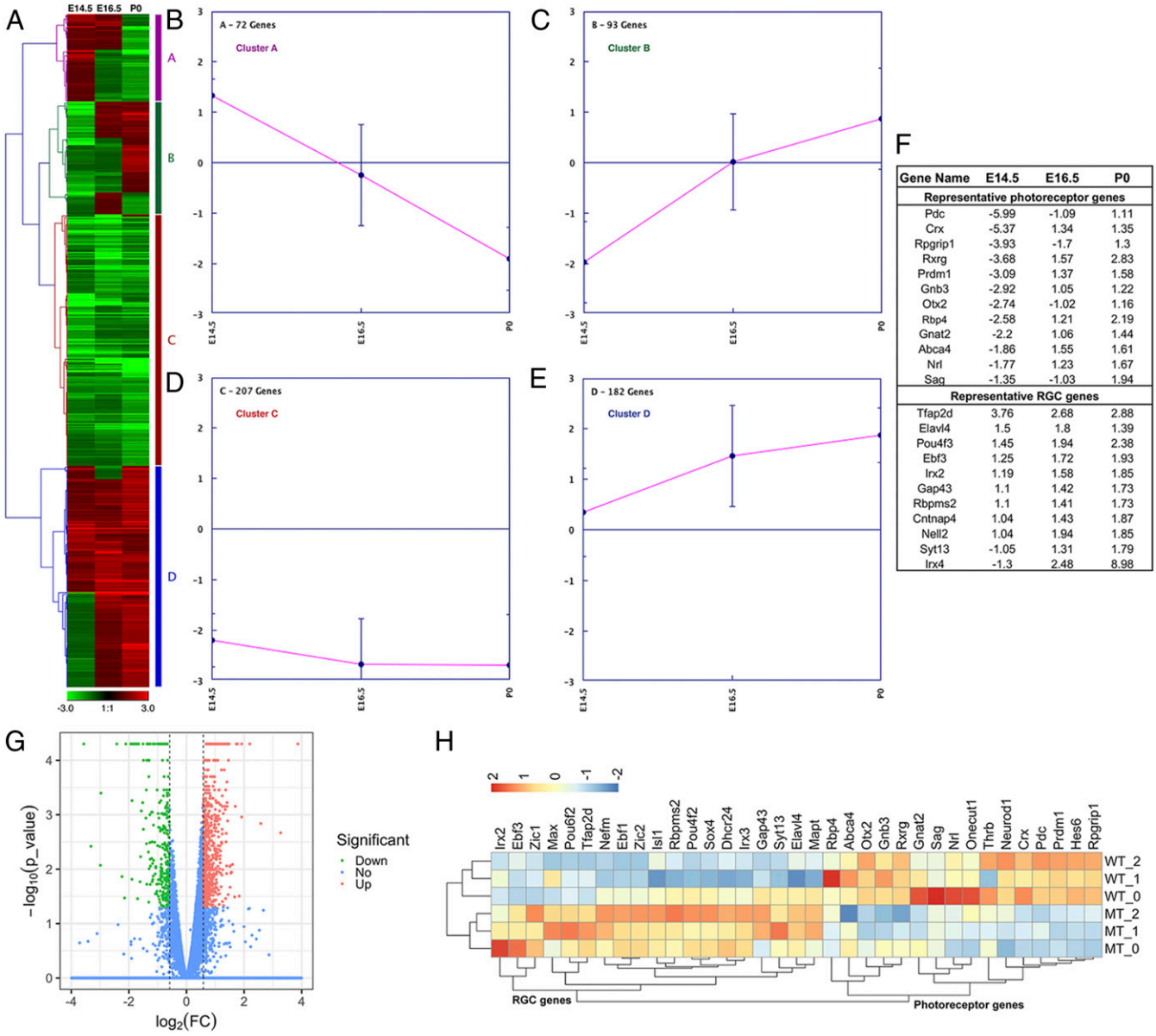

Gene Name	E14.5	E16.5	P0
Representative photoreceptor genes			
Pdc	-5.99	-1.09	1.11
Crx	-5.37	1.34	1.35
Rpgrip1	-3.93	-1.7	1.3
Rxrg	-3.68	1.57	2.83
Prdm1	-3.09	1.37	1.58
Gnb3	-2.92	1.05	1.22
Otx2	-2.74	-1.02	1.16
Rbp4	-2.58	1.21	2.19
Gnat2	-2.2	1.06	1.44
Abca4	-1.86	1.55	1.61
Nrl	-1.77	1.23	1.67
Sag	-1.35	-1.03	1.94
Representative RGC genes			
Tfap2d	3.76	2.68	2.88
Elavl4	1.5	1.8	1.39
Pou4f3	1.45	1.94	2.38
Ebf3	1.25	1.72	1.93
Irx2	1.19	1.58	1.85
Gap43	1.1	1.42	1.73
Rbpms2	1.1	1.41	1.73
Cntnap4	1.04	1.43	1.87
Nell2	1.04	1.94	1.85
Syt13	-1.05	1.31	1.79
Irx4	-1.3	2.48	8.98

Fig. 1. Aberrant temporal changes of Foxn4-dependent gene expression in *Foxn4*$^{lacZ/lacZ}$ retinas during development. (*A*) Hierarchical cluster analysis of Foxn4-dependent gene expression at E14.5, E16.5, and P0. The differentially expressed genes between *Foxn4*$^{lacZ/lacZ}$ and *Foxn4*$^{+/+}$ retinas were identified by microarray analysis at each stage. Fold changes are color-coded according to the bar (*Bottom*). This analysis yielded 4 major clusters: A to D. (*B–E*) Plots of the mean and normalized SD of expression of all genes in clusters A to D. (*F*) Fold changes (*Foxn4*$^{lacZ/lacZ}$ vs. *Foxn4*$^{+/+}$ retinas) in expression of representative photoreceptor genes and retinal ganglion cell genes at E14.5, E16.5, and P0. (*G*) Volcano plot (significance vs. fold change; FC) of significantly down-regulated (green) and up-regulated (red) genes (fold change > 1.5 and $P < 0.05$) between E14.5 wild-type and *Foxn4*$^{lacZ/lacZ}$ retinas, determined by RNA-seq analysis. (*H*) Heatmap of expression levels of representative photoreceptor and RGC genes between E14.5 *Foxn4* wild-type (WT) and mutant (MT) retinas, determined by RNA-seq analysis.

at the outer edge) from 4.8 to 8.7% and Nr2e3^{+} rods from 1.7 to 2.5% (Fig. 3 *H*, *I*, *L*, *M*, and *P*), indicating that Foxn4 is sufficient to promote the photoreceptor fate at early embryonic stages. However, if the electroporated retinas were cultured for 6 d (equivalent to ~P1 stage), we found that the proportions of rods and cones generated from transfected progenitors were both significantly decreased in retinas electroporated with pCIG-Foxn4 compared with the control (Fig. 3 *J*, *K*, and *N–P*), suggesting that forced Foxn4 expression inhibits photoreceptor generation instead of promoting it at postnatal stages. Indeed, we have shown previously that Foxn4 overexpression at P0 leads to suppression of photoreceptor differentiation (14). This result is consistent with the observed increase of photoreceptor production and photoreceptor marker expression in P0 *Foxn4*$^{lacZ/lacZ}$ retinas (14) (Fig. 1), and is caused by direct activation of Dll4-Notch signaling by Foxn4, which in turn inhibits the photoreceptor cell fate (17).

Inhibition of the Ganglion Cell Fate by Foxn4. Our cluster analysis of differentially expressed genes revealed that the genes in cluster D are mostly those whose expression is up-regulated in *Foxn4*-null retinas at all 3 tested stages (Fig. 1 *A* and *E*). Enriched in this cluster are many RGC-specific TF and marker genes including *Pou4f3*, *Ebf3*, *Irx2*, *Tfap2d*, *Gap43*, and *Nell2* (Fig. 1*F*), indicating RGC overproduction in *Foxn4*$^{lacZ/lacZ}$ retinas at E14.5, E16.5, and P0. In addition, RNA-seq analysis also identified a set

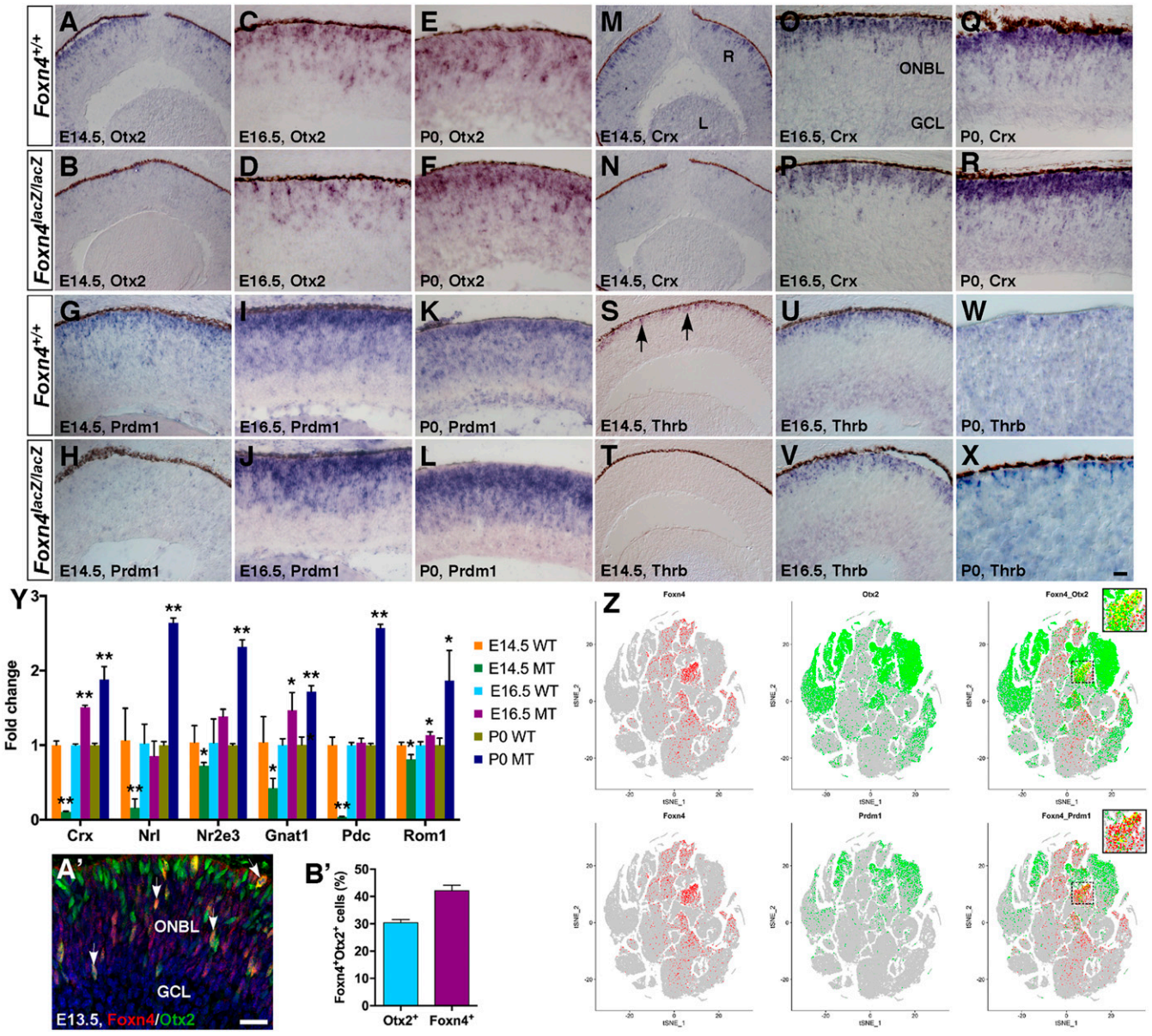

Fig. 2. Temporal alteration of photoreceptor gene expression in *Foxn4*$^{lacZ/lacZ}$ retinas. (*A*–*X*) Gene expression levels for *Otx2* (*A*–*F*), *Prdm1* (*G*–*L*), *Crx* (*M*–*R*), and *Thrb* (*S*–*X*) were examined by section RNA in situ hybridization analysis. All 4 genes display decreased expression at E14.5 but increased expression at P0 in *Foxn4*$^{lacZ/lacZ}$ retinas compared with the control. Arrows in *S* point to in situ hybridization signals. (Scale bar, 50 μm [*A*, *B*, *M*, and *N*], 25 μm [*C*–*L*, *O*–*R*, and *U*–*X*], and 100 μm [*S* and *T*].) (*Y*) Relative RNA levels of the indicated genes in *Foxn4* WT and mutant retinas, determined by qRT-PCR analysis. Each histogram represents the mean ± SD for triplicate samples. $*P < 0.05$, $**P < 0.001$. (*Z*) t-SNE plots of combined single retinal cells from E11 to P14 mice, colored by expression of the indicated genes. (*Z*, *Insets*) Corresponding outlined regions at a higher magnification. (*A*′ and *B*′) The presence of Foxn4$^+$Otx2$^+$ double-immunoreactive cells in E13.5 WT retinas (*A*′) and their quantification (*B*′). Arrows point to representative colocalized cells. (Scale bar, 20 μm [*A*′].) GCL, ganglion cell layer; L, lens; ONBL, outer neuroblastic layer; R, retina.

of RGC marker genes (e.g., *Rbpms2*, *Nefm*, *Irx3*, *Zic1*, *Tfap2d*, and *Mapt*) which are up-regulated in *Foxn4*$^{lacZ/lacZ}$ retinas (Fig. 1*H*). Thus, loss of *Foxn4* function may cause a fate switch in progenitors to produce more RGCs. Consistent with this, we found that the number of Pou4f1/Brn3a-immunoreactive RGCs in E14.5 *Foxn4*$^{lacZ/lacZ}$ retinas nearly doubled compared with those in control retinas (Fig. 4 *A*–*C*). Similarly, in E15.5 *Foxn4*$^{lacZ/lacZ}$ retinas, Rxrg-immunoreactive RGCs located in the ganglion cell layer were obviously increased (Fig. 3 *A* and *B*).

The increased RGCs in mutant retinas suggest that Foxn4 normally would inhibit RGC fate during retinal development. To test this speculation, we overexpressed Foxn4 in E13.5 retinal explants using a replication-incompetent murine retroviral vector that carries a green fluorescent protein (GFP) reporter (14) (Fig. 4*D*). The infected retinas were harvested after 4.5 d in culture to analyze the differentiation of RGCs and horizontal cells. We found that overexpressed Foxn4 decreased Pou4f1$^+$ RGCs by almost 3-fold but increased Lhx1$^+$ horizontal cells by ∼4-fold (Fig. 4 *E*, *F*, and *H*–*J*), suggesting that Foxn4 has an intrinsic activity to suppress the RGC fate. Consistent with previous results (34), overexpressed Ptf1a also greatly reduced Pou4f1$^+$ RGCs (Fig. 4 *D*, *E*, and *G*). Given our previous findings that Ptf1a acts downstream of Foxn4 and inhibits RGC differentiation by suppressing the expression of RGC TF genes *Atoh7* and *Pou4f2* (28), Foxn4 appears to inhibit RGC fate by activating *Ptf1a* expression (Fig. 4*K*).

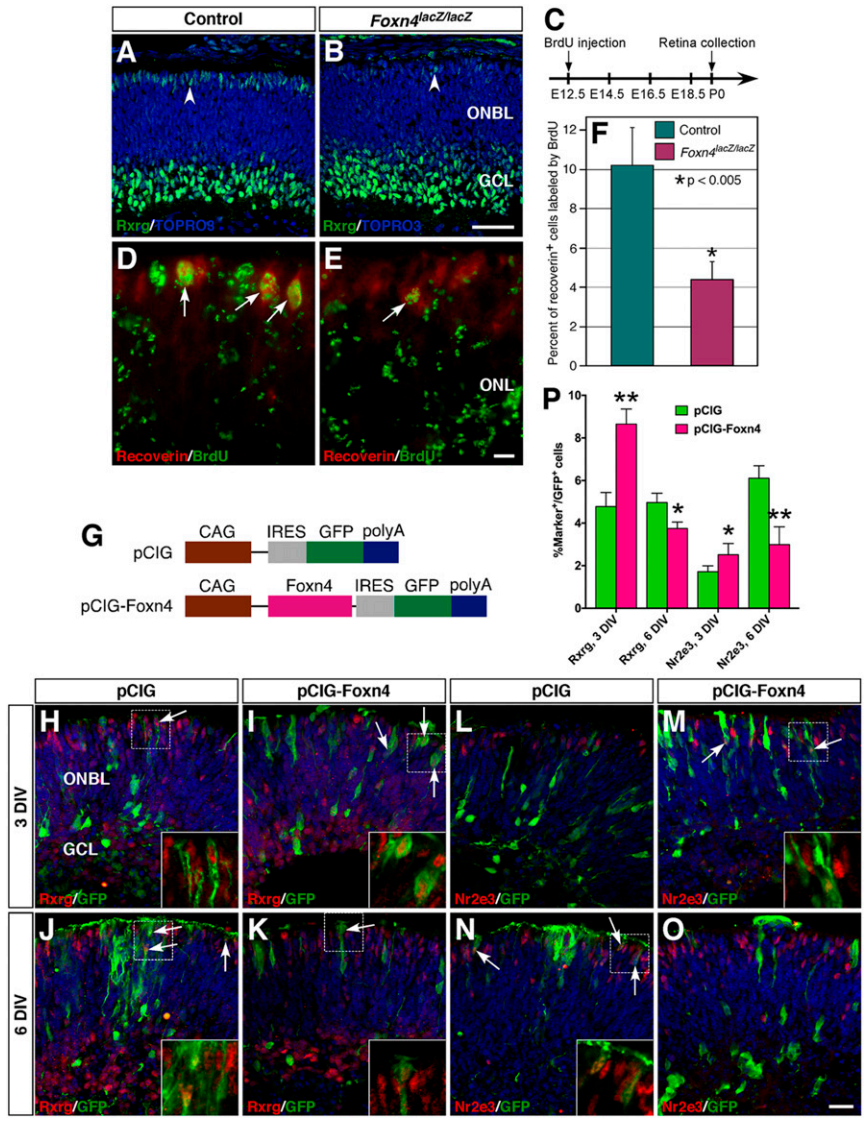

Fig. 3. Abnormal photoreceptor generation caused by *Foxn4* inactivation and overexpression. (*A* and *B*) Rxrg-immunoreactive cones (indicated by the arrowheads) were dramatically reduced in E15.5 *Foxn4*$^{lacZ/lacZ}$ retinas even though Rxrg^{+} RGCs were increased. (Scale bar, 39.7 μm.) (*C*) Schematic of the BrdU-labeling schedule during retinal development. (*D* and *E*) Control and mutant retinas were pulse-labeled by BrdU at E12.5 and analyzed by double immunofluorescence for BrdU and recoverin at P0. Arrows point to colabeled cells which decreased in *Foxn4*$^{lacZ/lacZ}$ retinas. (Scale bar, 5 μm.) (*F*) Quantitation of recoverin-immunoreactive cells that were colabeled with BrdU. Each histogram represents the mean ± SD for 4 retinas. *$P < 0.005$. (*G*) Schematic of the pCIG and pCIG-Foxn4 expression plasmids. (*H–O*) E13.5 retinas electroporated ex vivo with pCIG or pCIG-Foxn4 DNA were collected after culture for 3 d (DIV) or 6 d, and then their sections were double-immunostained with an anti-GFP antibody and antibodies against Rxrg or Nr2e3 and counterstained with nuclear DAPI. Arrows point to representative colocalized cells. (*H–O*, *Insets*) Corresponding outlined regions at a higher magnification. (Scale bar, 20 μm.) (*P*) Quantitation of GFP^{+} cells that become immunoreactive for Rxrg or Nr2e3 at the outer edge of the retina. Each histogram represents the mean ± SD for 3 or 4 retinas. *$P < 0.05$, **$P < 0.01$. ONL, outer nuclear layer.

Opposing Regulatory Effects of Foxn4 on *Ikzf1* and *Casz1* Expression. Our experimental results together with our early work reveal that Foxn4 can bias RPCs toward cone, rod, amacrine, and horizontal cells rather than to a particular cell fate, just as the tTFs Ikzf1 and Casz1 do (12–14), suggesting that Foxn4 may also act as a tTF. In *Drosophila* cascades of tTFs, one tTF activates the next tTF while repressing the previous one to facilitate temporal transitions in neuroblasts (10). We therefore investigated whether Foxn4 would regulate the expression of *Ikzf1* and *Casz1* in RPCs. qRT-PCR assay showed that in *Foxn4*$^{lacZ/lacZ}$ retinas, *Ikzf1* expression was significantly up-regulated at E14.5 and E16.5 but not at P0 while *Casz1* expression was significantly down-regulated at E16.5 and P0 but not E14.5 (Fig. 5*A*), suggesting timing-dependent repression of *Ikzf1* but activation of *Casz1* by Foxn4 in RPCs. To confirm these regulatory relationships, we electroporated pCIG-Foxn4 and pCIG plasmid DNA into P0 mouse retinas and purified transfected GFP^{+} cells at P4 by FACS (fluorescence-activated cell sorting) (Fig. 5*B*). In these purified cells, qRT-PCR assay showed that *Ikzf1* expression was significantly down-regulated whereas *Casz1* expression was significantly up-regulated by Foxn4 overexpression (Fig. 5*C*). Consistent with these results, analysis of scRNA-seq data of murine retinal cells from stages E11 to P14 (33) showed that there was no colocalization between *Ikzf1* and *Foxn4* in RPCs whereas *Casz1* was coexpressed with *Foxn4* in many single RPCs (Fig. 5*D*). Stage-specific analysis similarly revealed colocalization between *Foxn4* and *Casz1* but not *Ikzf1* at embryonic stages (*SI Appendix*, Fig. S3). Moreover, fluorescence in situ hybridization showed that many *Foxn4* and *Casz1* signals were juxtaposed to one another and some overlapped in E14.5 retinas (Fig. 5 *E* and *F*), consistent with coexpression of *Foxn4* and *Casz1* in the same cells. Thus, Foxn4 appears to directly and/or indirectly repress *Ikzf1* expression but activate *Casz1* expression in RPCs in a stage-dependent manner.

Conditional Ablation of *Foxn4* in the Retina. Conventional *Foxn4* knockout in mice results in a lethal phenotype during neonatal and early postnatal stages (14), precluding further analysis of the retinal phenotype at later stages. To circumvent this issue, we generated mice with a floxed allele of *Foxn4* by homologous recombination in embryonic stem (ES) cells as well as by breeding targeted animals with the FLPeR transgenic line (35) to remove the neomycin selection marker gene (*SI Appendix*, Fig. S4). Further breeding between floxed mice and the Six3-Cre driver transgenic line (36) led to efficient retina-specific deletion of the second coding exon of *Foxn4* (*SI Appendix*, Figs. S4 and S5).

Homozygous conditional knockout *Foxn4*$^{\Delta fl/\Delta fl}$ mice appeared to survive normally. In 3-mo-old *Foxn4*$^{\Delta fl/\Delta fl}$ retinas, immunofluorescence staining revealed near-complete loss of horizontal

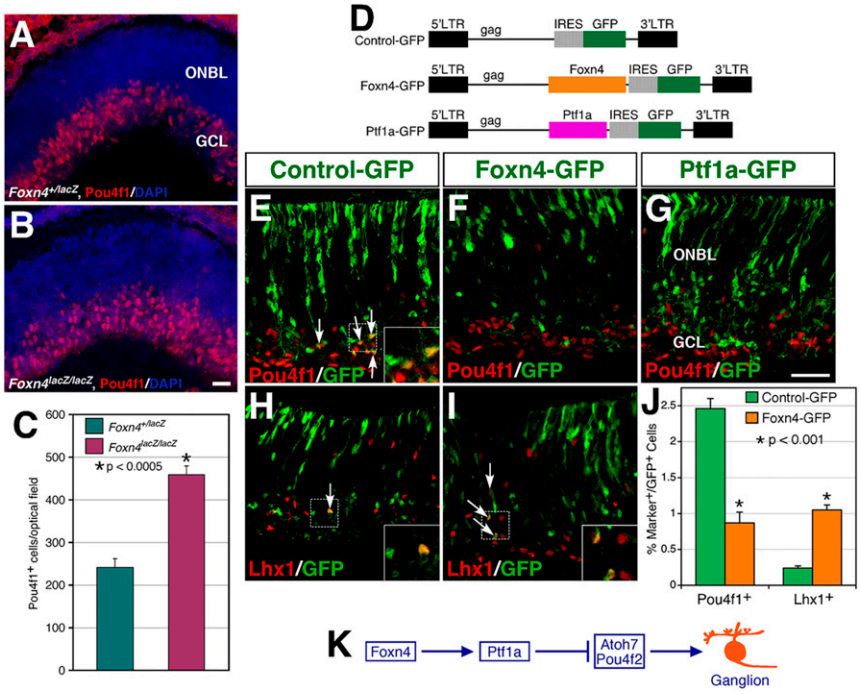

Fig. 4. Inhibition of RGC specification by Foxn4. (*A* and *B*) Increased Pou4f1-immunoreactive RGCs in E14.5 *Foxn4*$^{lacZ/lacZ}$ retinas compared with the control. (*C*) Quantification of Pou4f1-immunoreactive cells in E14.5 *Foxn4*$^{lacZ/lacZ}$ and *Foxn4*$^{+/lacZ}$ retinas. Each histogram represents the mean ± SD for 3 retinas. *$P < 0.0005$. (*D*) Schematics of control-GFP, Foxn4-GFP, and Ptf1a-GFP retroviral constructs. The internal ribosomal entry site (IRES) allows for simultaneous expression of 2 proteins. (*E–I*) Sections from retinas infected with control-, Foxn4-, or Ptf1a-GFP viruses at E13.5 were double-immunostained with an anti-GFP antibody and antibodies against Pou4f1 or Lhx1. Overexpressed Foxn4 significantly decreased Pou4f1-immunoreactive RGCs but increased horizontal cells immunoreactive for Lhx1. Forced Ptf1a expression similarly reduced Pou4f1-immunoreactive RGCs. Arrows point to representative colocalized cells. (*E–I*, *Insets*) Corresponding outlined regions at a higher magnification. (*J*) Quantification of virus-transduced retinal cells that become immunoreactive for Pou4f1 or Lhx1. Each histogram represents the mean ± SD for 3 retinas. *$P < 0.001$. (*K*) Model indicating how Foxn4 may suppress the RGC fate by activating *Ptf1a* expression which in turn represses the expression of RGC specification TF factors Atoh7 and Pou4f2. (Scale bars, 25 μm [*A* and *B*] and 39.7 μm [*E–I*].)

cells immunoreactive for Lhx1 and calbindin and significant reduction of amacrine cells immunoreactive for Pax6, calretinin, or GAD65 (Fig. 6 *A–J* and *U*), in agreement with the observed developmental defects in the conventional knockout retinas (14). Compared with control retinas, there appeared to be no significant change in the number of Chx10^{+} bipolar cells, Pou4f1^{+} RGCs, Sox9^{+} Müller cells, and cone cells positive for cone opsin and arrestin in conditional mutant retinas (Fig. 6 *K–U*).

Retinal Degeneration and Electroretinogram Defects in Conditional *Foxn4*-Null Mice. It has been shown previously that ablation of horizontal cells or failure to develop them leads to retinal degeneration (37–39). The observed horizontal cell loss thus suggests a possibility of degeneration of *Foxn4*$^{\Delta fl/\Delta fl}$ retinas. To assess this possibility, we stained retinal sections from 1.5-, 3-, and 6-mo-old mice with hematoxylin-eosin. This histochemical analysis revealed a progressive degeneration of the mutant retina. At 1.5 and 3 mo of age, although the *Foxn4*$^{\Delta fl/\Delta fl}$ retina still had a typical laminar organization containing all of the cellular layers, compared with the control, it was obviously reduced in thickness, especially in the inner nuclear layer, outer and inner plexiform layers, and ganglion cell layer (Fig. 7 *A–D*). By 6 mo, all layers of the mutant retina including the outer nuclear layer were further decreased in thickness and the outer plexiform layer became obscure (Fig. 7 *E* and *F*).

To evaluate the visual function of the mutant mice, we recorded ERG (electroretinogram) responses from 3-mo-old control and *Foxn4*$^{\Delta fl/\Delta fl}$ animals. Under dark-adapted conditions (Fig. 7*G*), for low flash intensities (bottom 3 pairs of traces), ERG responses were dominated by the "b" wave, and mutant mice consistently showed lower response amplitudes than those elicited from wild-type animals. For higher-intensity flashes (top 4 pairs of traces), "a" waves were visible for both wild-type and mutant animals. Compared with control mice, large reductions in scotopic b-wave amplitudes (~60%) were observed in mutants (Fig. 7*J*). *Foxn4*$^{\Delta fl/\Delta fl}$ mice also exhibited a decrease in the amplitude of photopic ERG responses. Fig. 7*H* shows typical ERG waveforms obtained from 3-mo-old control and mutant mice. Similar to dark-adapted ERG responses, mutant animals displayed about 60% reduction in b-wave amplitudes in light-adapted ERG (Fig. 7*K*). However, unlike b waves, both scotopic and photopic a waves showed no significant difference in amplitude between control and mutant animals (Fig. 7*I* and *SI Appendix*, Fig. S6). ERG responses were also recorded from 7-mo-old control and *Foxn4*$^{\Delta fl/\Delta fl}$ animals and we found that the mutant mice exhibited ERG response defects similar to those of 3-mo-old *Foxn4*$^{\Delta fl/\Delta fl}$ animals (*SI Appendix*, Fig. S7). Moreover, in agreement with the observed age-dependent progressive retinal degeneration (Fig. 7 *A–F*), the amplitude reduction of scotopic a waves in mutant animals became pronounced and significant compared with that at 3 mo (Fig. 7*I* and *SI Appendix*, Fig. S7*C*).

Aberrant Synaptogenesis in Conditional *Foxn4*-Null Retinas. The horizontal cell loss may result in defective synaptic connections in the retina (38, 39), which would cause anomalous ERG responses in *Foxn4*$^{\Delta fl/\Delta fl}$ animals. Indeed, in 1.5-mo-old *Foxn4*$^{\Delta fl/\Delta fl}$ retinas, there were fewer synaptic ribbons immunoreactive for Bassoon or Ribeye in the outer plexiform layer (OPL) compared with control retinas (Fig. 8 *A–D*). Peanut agglutinin (PNA) labeling revealed that flat contacts between cones and cone bipolar cells were similarly decreased within the OPL in the mutant retina (Fig. 8 *E* and *F*). In addition, in the *Foxn4*$^{\Delta fl/\Delta fl}$ retina, there was diminished expression of synaptophysin, which is a presynaptic vesicle marker (Fig. 8 *G* and *H*). Horizontal cell ablation was shown to cause retraction of rod spherules from the OPL and formation of ectopic synapses between retracted spherules with rod bipolar cells in the outer nuclear layer (39). Consistent with this, we found that in *Foxn4*$^{\Delta fl/\Delta fl}$ retinas, rod bipolar cells immunoreactive for protein kinase Cα sprouted dendrites into the outer nuclear layer, which were absent from control retinas (Fig. 8 *I* and *J*). In 3-mo-old *Foxn4*$^{\Delta fl/\Delta fl}$ retinas, we observed similar abnormal immunolabeling patterns for Bassoon, Ribeye, PNA, synaptophysin, and protein kinase Cα (*SI Appendix*, Fig. S8), indicating a synaptogenic defect and/or loss of synaptic connections in the mutant retina.

We investigated further the synaptogenic defects in *Foxn4*$^{\Delta fl/\Delta fl}$ retinas by transmission electron microscopy. At 3 mo of age, the OPL of the mutant retina became narrower and irregularly shaped (Fig. 8 *K* and *L*), in agreement with its age-dependent collapse observed in the *Foxn4*$^{\Delta fl/\Delta fl}$ retina (Fig. 7 *A–F*). In control retinas, the invaginating synapses exhibited a typical triad structure consisting of a presynaptic ribbon, 2 lateral dendrites of horizontal cells, and 1 centrally oriented dendrite of the bipolar cell (Fig. 8*M*). By contrast, most of these synapses became deformed to varying degrees

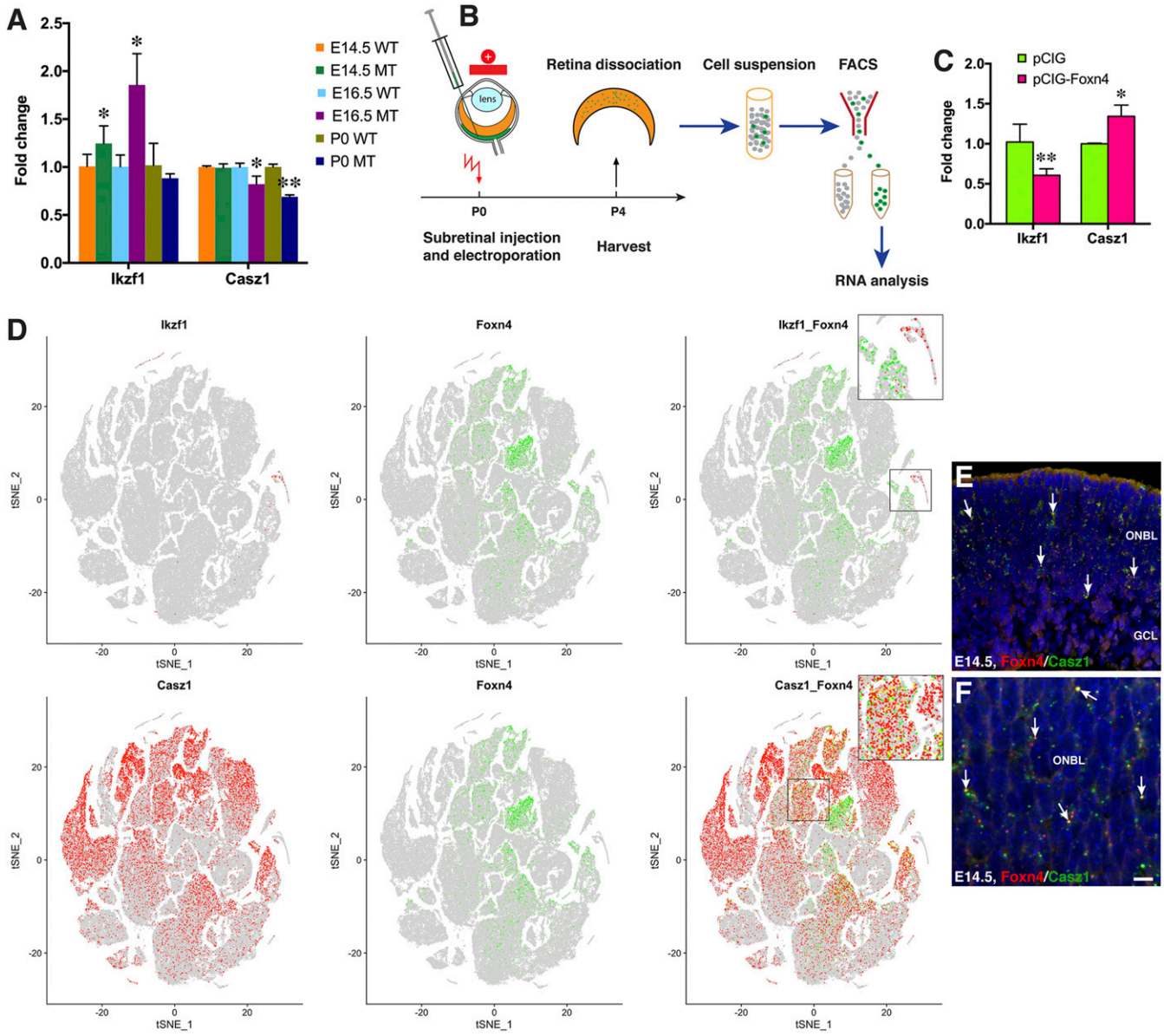

Fig. 5. Regulation of *Ikzf1* and *Casz1* expression by Foxn4. (*A*) Relative RNA levels of *Ikzf1* and *Casz1* in *Foxn4* WT and mutant retinas, determined by qRT-PCR analysis. Each histogram represents the mean ± SD for 3 to 6 samples. $*P < 0.05$, $**P < 0.0001$. (*B*) Schematic of the procedure for retinal overexpression and isolation of transfected GFP$^+$ cells by FACS. (*C*) Relative RNA levels of *Ikzf1* and *Casz1* in GFP$^+$ cells transfected with pCIG-Foxn4 or pCIG control plasmid DNA, determined by qRT-PCR analysis. Each histogram represents the mean ± SD for 3 samples. $*P < 0.05$, $**P < 0.005$. (*D*) t-SNE plots of combined single retinal cells from E11 to P14 mice, colored by expression of the indicated genes. (*D*, *Insets*) Corresponding outlined regions at a higher magnification. (*E* and *F*) *Foxn4* and *Casz1* expression was examined by fluorescence in situ hybridization analysis of E14.5 WT retinal sections. Arrows point to representative overlapped signals. (Scale bar, 15 μm [*E*] and 6.3 μm [*F*].)

without the typical triad configuration in *Foxn4*$^{\Delta fl/\Delta fl}$ retinas (Fig. 8 *N*–*P*). In extreme cases, the presynaptic ribbons failed to be anchored to the membrane and became "free-floating" (Fig. 8 *N* and *O*). In addition, swollen mitochondria were occasionally seen in the mutant retina (Fig. 8*N*). Therefore, conditional *Foxn4* inactivation results in a severe synaptogenic defect in the murine retina.

Discussion

Foxn4 Acts as a tTF to Confer Retinal Progenitors with the Competence to Generate Cone, Rod, Amacrine, and Horizontal Cells. In our previous work, we have shown that Foxn4 is expressed in retinal progenitors, confers them with the competence to generate amacrine and horizontal cells, and inhibits the photoreceptor cell fates in neighboring progenitors at neonatal stages (14, 17). Unexpectedly, however, we find in this study that Foxn4 is a facilitator of the photoreceptor cell fate during early retinogenesis. In E14.5 *Foxn4* mutant retinas, temporal cluster analysis, RNA-seq analysis, RNA in situ hybridization, qRT-PCR assay, and immunostaining all revealed that there was a significant down-regulation of a number of TF genes, such as *Otx2*, *Crx*, *Nrl*, *Nr2e3*, *Thrb*, *Prdm1*, and *Rxrg*, which are involved in photoreceptor cell specification and differentiation (7, 32, 40). Furthermore, BrdU-labeling experiments confirmed decreased generation of photoreceptors in E12.5 *Foxn4* mutant retinas whereas forced Foxn4 expression promoted their generation in early embryonic retinas. Therefore, apart from conferring RPCs with the competence to generate amacrine and horizontal

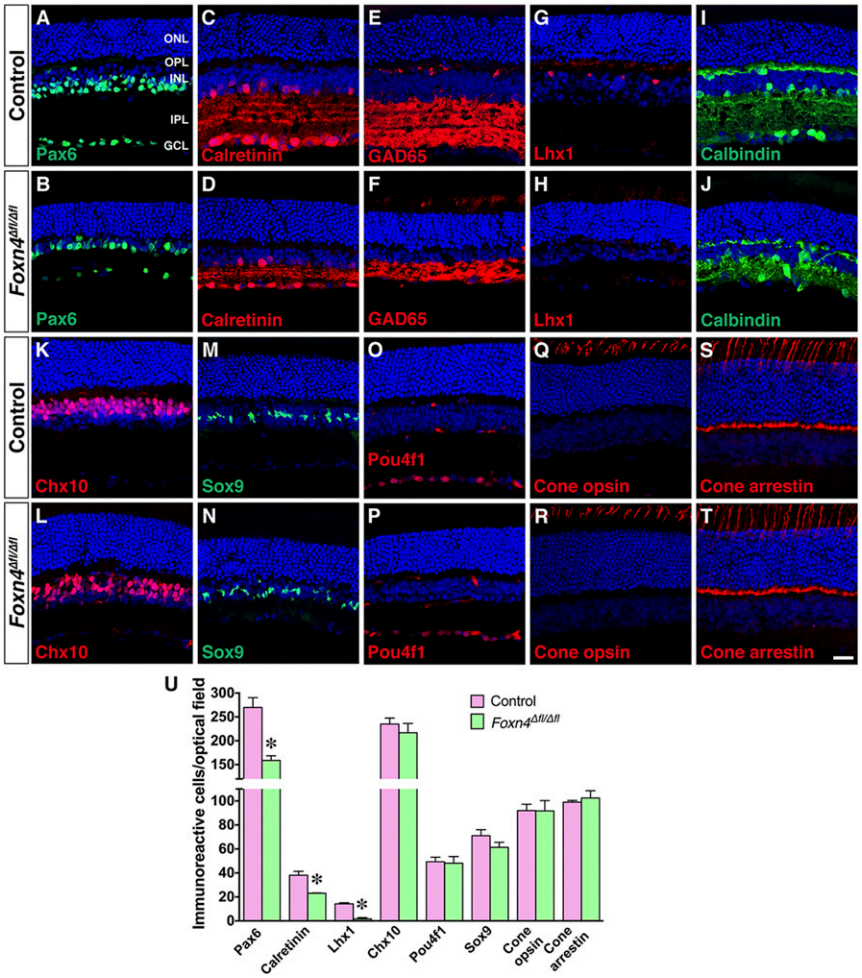

Fig. 6. Effect of conditional *Foxn4* ablation on differentiation of different retinal cell types. (*A*–*T*) Retinal sections from 3-mo-old control and $Foxn4^{\Delta fl/\Delta fl}$ mice were immunostained with antibodies against the indicated cell type-specific markers and weakly counterstained with nuclear DAPI. *Foxn4* inactivation resulted in a decrease of amacrine cells immunoreactive for Pax6, calretinin, GAD65, or calbindin (*A*–*F*, *I*, and *J*) and horizontal cells immunoreactive for Lhx1 and calbindin (*G*–*J*), but no obvious changes in $Chx10^+$ bipolar cells, $Sox9^+$ Müller cells, $Pou4f1^+$ RGCs, or cones positive for cone opsins (M and S opsins) or cone arrestin (*K*–*T*). (*U*) Quantitation of cells that are immunoreactive for several cell type-specific markers. Each histogram represents the mean ± SD for 3 or 4 retinas. $^*P < 0.005$. GCL, ganglion cell layer; INL, inner nuclear layer; IPL, inner plexiform layer; ONL, outer nuclear layer; OPL, outer plexiform layer. (Scale bar, 20 μm.)

cells, Foxn4 appears to also be involved in conferring the progenitors with the competence to generate cones and rods at early embryonic stages (Fig. 9).

In vertebrates, unlike in *Drosophila*, tTFs have been shown to bias the cell-fate decision of progenitors rather than specifying rigidly one cell fate (5, 9). Thus, Foxn4 well qualifies as a tTF because of its property of biasing RPCs toward cone, rod, amacrine, and horizontal cells instead of specifying a particular cell fate, as well as its temporally transient expression pattern in progenitors (14). Previous studies have implied that a putative cascade of tTFs similar to those operating in *Drosophila* neuroblasts may exist in mammalian RPCs to confer their temporal identities during retinogenesis (8, 12, 13). Ikzf1 has been shown to confer RPCs with the competence to generate immediate-early cell types: RGCs, and horizontal and amacrine cells, and Casz1 with the competence to generate mid/late cell types including rod and bipolar cells (12, 13). However, at least 2 tTFs must be missing from this putative tTF cascade: One is responsible for biasing RPCs toward cones, which is an early-born cell fate, and another for biasing RPCs toward Müller cells, which is a late-born cell fate (Fig. 9*A*). In this study, we provide evidence to show that Foxn4 is able to confer RPCs with the competence to generate not only amacrine and horizontal cells but also cones and rods, suggesting that Foxn4 may function as a tTF, which can be placed between Ikzf1 and Casz1 to bias RPCs toward mid/late-early cell fates: horizontal, amacrine, cone, and rod cells. Additionally, our data indicate a possibility that Foxn4 may activate *Casz1* expression while repressing *Ikzf1* expression in RPCs (Fig. 9*A*). Thus, we have identified a tTF missing from the cascade that controls RPC temporal identities during mammalian retinal development. The addition of Foxn4 to this cascade implies that this mammalian temporal cascade unlikely consists of all homologs of the *Drosophila* VNC tTFs, despite the fact that Ikzf1 and Casz1 are orthologs of VNC tTFs Hunchback and Castor, respectively (12, 13). Nevertheless, there are at least 2 Fox TFs that participate in *Drosophila* tTF cascades: Sloppy-paired 1 and 2 in the medulla neuroblasts of the developing optic lobe (41).

At around neonatal stages, we found that a number of photoreceptor TF and marker genes were up-regulated in *Foxn4*-null retinas, consistent with our earlier findings (14), suggesting that Foxn4 suppresses the photoreceptor fate at later developmental stages. How to explain this seemingly paradoxical phenomenon? We believe that it manifests the balanced outcome of two opposing effects exerted by Foxn4 on photoreceptor development. On the one hand, as discussed above, Foxn4 has an intrinsic activity to confer RPCs with the competence to generate cones and rods by directly and/or indirectly activating the expression of photoreceptor determination and differentiation TFs such as Otx2, Crx, Nrl, and Prdm1 (Fig. 9*B*). On the other hand, as we have shown previously (17), Foxn4 can directly activate Dll4-Notch signaling, which serves as an extrinsic signal to repress the expression of these photoreceptor TFs in neighboring progenitor cells (Fig. 9*B*). During retinogenesis, as progenitor competence gradually shifts from early to late states, the presumptive molecular (e.g., accumulating Notch expression), epigenetic, and microenvironmental changes accompanied by the competence state switch may make RPCs more conducive for Dll4-Notch signaling, resulting in a net effect of photoreceptor fate inhibition rather than promotion. In agreement with this idea, Foxn4 overexpression inhibits photoreceptor generation at around

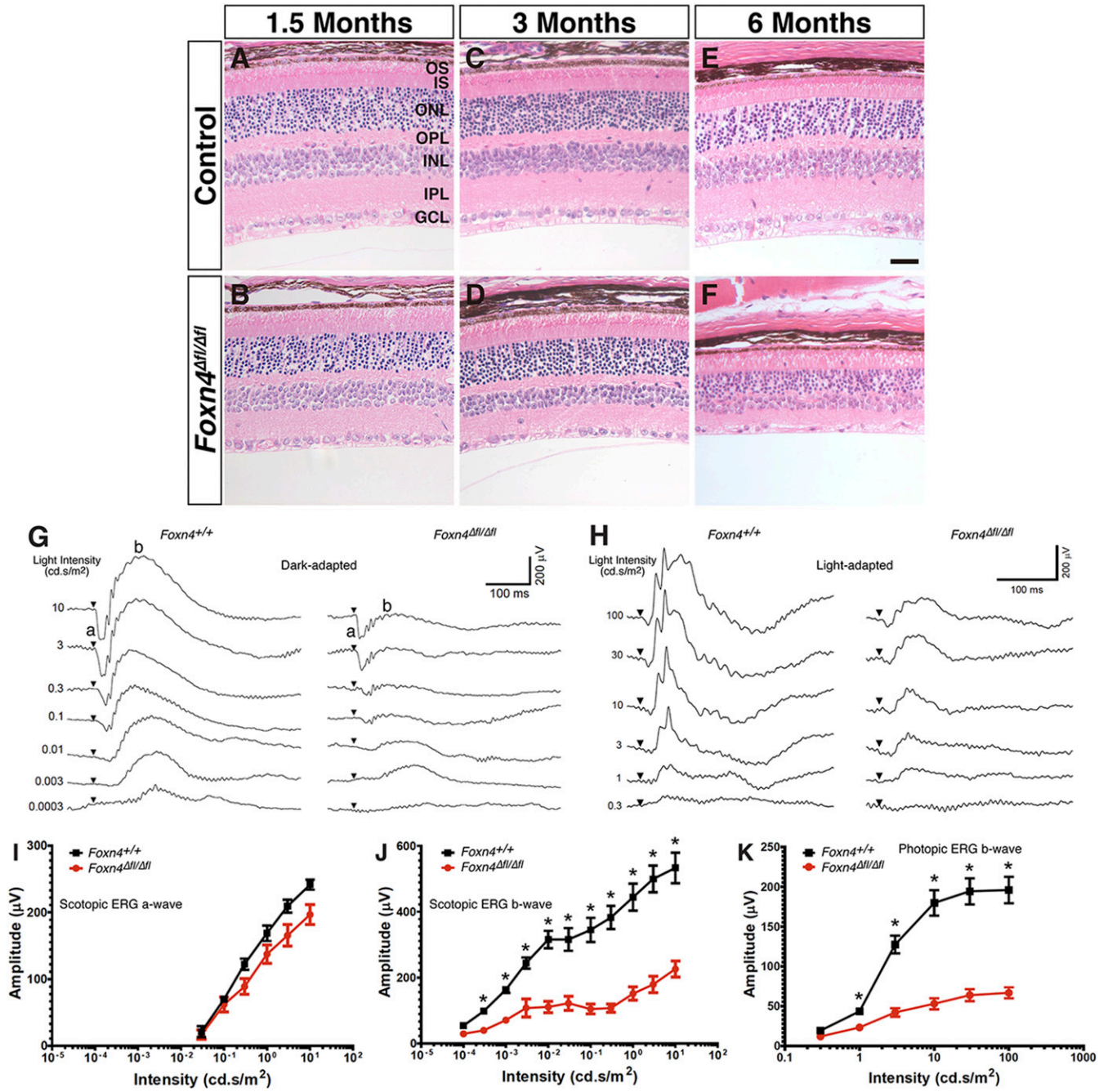

Fig. 7. Alterations in retinal structure and ERG response in *Foxn4*$^{\Delta fl/\Delta fl}$ mice. (*A*–*F*) Laminar structures were visualized in 1.5-, 3-, and 6-mo-old retinal sections by hematoxylin-eosin staining. Compared with the control, there is a progressive decrease in the thickness of the *Foxn4*$^{\Delta fl/\Delta fl}$ retina. (*G* and *H*) Representative ERG waveforms from dark-adapted (*G*) and light-adapted (*H*) control and mutant animals of 3 mo of age. The flash intensity used to elicit the responses is given to the left of each pair of responses, and the inverted triangles indicate the onset of the light stimuli. (*I*–*K*) Intensity–response functions of scotopic ERG a waves (*I*) and b waves (*J*) and photopic ERG b waves (*K*) for WT and mutant mice. Data are presented as mean ± SEM (WT, $n = 8$; mutant, $n = 10$). Asterisks indicate significance in a two-way ANOVA test with the Bonferroni correction: $^*P < 0.01$ (*J* and *K*). IS, inner segment; OS, outer segment. (Scale bar, 20 μm.)

neonatal stages but promotes it at early embryonic stages (14) (Fig. 3). The opposing effects of Foxn4 may also serve as a safeguard mechanism to prevent overproduction of photoreceptors and to ensure generation of appropriate numbers of different retinal cell types. Conceivably, although early RPCs need Foxn4 to acquire the photoreceptor generation competence, due to the down-regulation of Foxn4 expression as development progresses (14), later RPCs may acquire Foxn4-independent competence of photoreceptor generation because of the change of competence states.

The coexpression of *Foxn4* and *Otx2* in a subset of RPCs, revealed by scRNA-seq and immunolabeling analyses, suggests a possibility that early *Otx2* expression may be directly activated by Foxn4. On the other hand, given the limited or lack of colocalization between *Foxn4* and *Prdm1*, *Crx*, *Nrl*, *Nr2e3*, *Thrb*, or *Rxrg*, it is unlikely for these other photoreceptor regulatory TF genes to be directly activated by Foxn4. Nevertheless, it has been shown that Otx2 sits at the top of the gene regulatory network governing photoreceptor specification and differentiation and that all other photoreceptor regulatory TF genes are down-regulated in

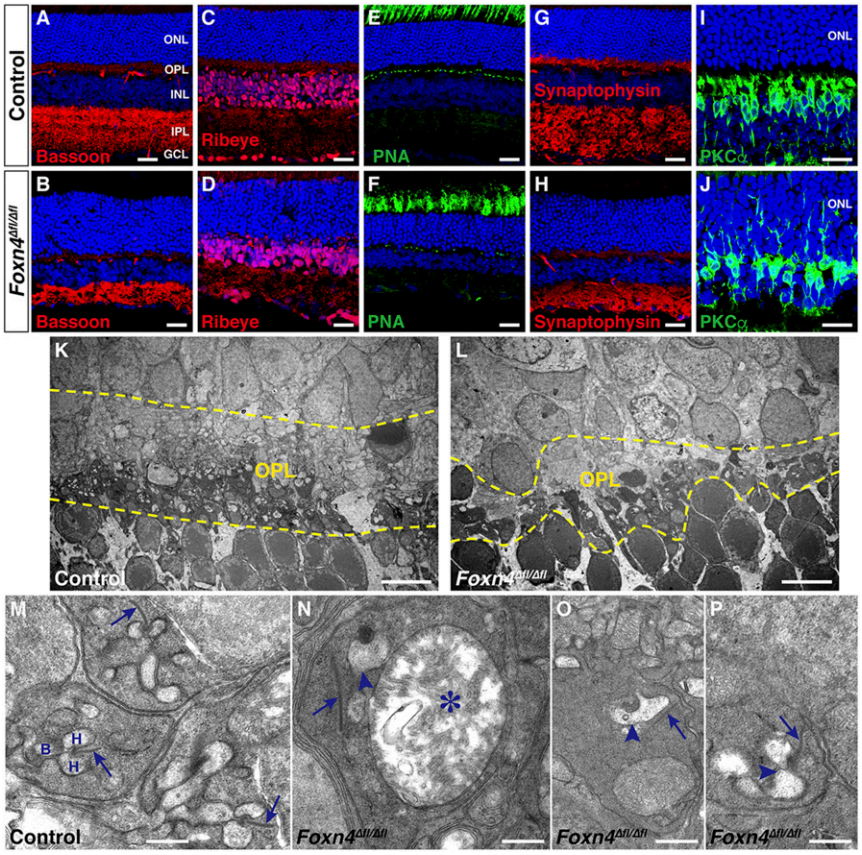

Fig. 8. Synaptogenic defects in the outer plexiform layer of *Foxn4*$^{\Delta fl/\Delta fl}$ retinas. (*A–J*) Retinal sections from 1.5-mo-old control and *Foxn4*$^{\Delta fl/\Delta fl}$ mice were immunostained with the indicated antibodies and weakly counterstained with nuclear DAPI. In the mutant retina, note the reduced labeling in the OPL for Bassoon, Ribeye, PNA, and synaptophysin and extension of PKCα-immunoreactive rod bipolar cell dendrites into the ONL. (*K* and *L*) Transmission electron microscopy images of the OPL of retinas from 3-mo-old control and *Foxn4*$^{\Delta fl/\Delta fl}$ mice. The mutant OPL is narrower and irregularly shaped. Dotted lines indicate the OPL boundaries. (*M–P*) High-magnification images of control and mutant photoreceptor terminals. The control invaginating synapses have a typical triad ultrastructure composed of a presynaptic ribbon, 2 horizontal cell (marked as H) processes, and a bipolar cell (marked as B) dendrite (*M*), whereas those in the mutant lack the triad morphology (*N–P*). Unanchored free-floating ribbons can often be seen in mutant terminals (*N* and *O*). The arrows indicate presynaptic ribbons and arrowheads indicate deformed synapses. The asterisk indicates a swollen mitochondrion. (Scale bars, 20 μm [*A–J*], 5 μm [*K* and *L*], and 0.5 μm [*M–P*].)

the absence of *Otx2* (32, 40, 42). Therefore, Foxn4 may indirectly regulate the expression of the rest of the photoreceptor TF genes by directly activating *Otx2* expression first. It will be interesting to delineate the direct or indirect regulatory relationships between Foxn4 and all photoreceptor regulatory TFs in future mechanistic studies.

Foxn4 Suppresses RGC Generation Competence in Retinal Progenitors. Although there are discrepancies among different models that explain retinal cell development, it is agreed that there is a pool of early RPCs which give rise to early-born cell types including amacrine, horizontal, ganglion, and cone cells as well as a small number of early-born rod cells. RPCs biased toward the RGC fate generate fewer amacrine, horizontal, and photoreceptor cells, and vice versa. This type of "binary" fate choice model has been widely verified in neural development of the spinal cord, retina, and brain. It is therefore conceivable that Foxn4 would suppress the competence of RGC generation as a result of its activity to bias early RPCs toward the amacrine, horizontal, and photoreceptor cell fates. Indeed, we have shown in this work that this is the case: 1) Bioinformatic analyses revealed up-regulation of many RGC marker genes at different developmental stages in *Foxn4*-null retinas; 2) immunostaining assay showed a significant increase of RGCs generated in *Foxn4*-null retinas at early stages; and 3) overexpression experiments demonstrated inhibition of RGC generation by Foxn4. It should be pointed out that the increase of RGC population in *Foxn4*-null retinas is temporary, and eventually the number of RGCs is restored to normal, likely due to elevated apoptosis (14) (Fig. 6).

Our data suggest that one mechanism by which Foxn4 inhibits RGC competence is by directly activating Ptf1a expression, which in turn suppresses the expression of RGC specification and differentiation TFs Atoh7 and Pou4f2 (43–48) (Fig. 9*B*). In previous studies, Foxn4 has been shown to bind directly to a *Ptf1a* enhancer and act synergistically with RORβ1 to activate the expression of *Ptf1a* (27). Correspondingly, *Foxn4* deficiency results in near-complete down-regulation of *Ptf1a* expression (28). Ptf1a has been shown to inhibit RGC fate because its inactivation causes an increase of RGCs whereas its overexpression reduces RGCs (28, 34, 49) (Fig. 4). Since *Ptf1a* inactivation leads to up-regulation of *Atoh7* and *Pou4f2* expression (28, 49), it appears to inhibit RGC generation by suppressing the expression of these 2 RGC regulatory TF genes. In addition, our current and previous RNA-seq, microarray, and in situ hybridization analyses have all demonstrated significant down-regulation of *Neurod4* and *Neurod1* expression in *Foxn4*-null retinas (14, 17). Given that *Neurod4* and *Neurod1* double knockout in mice causes increased RGC generation and concomitant up-regulation of *Atoh7* expression (50), these 2 basic helix-loop-helix (bHLH) TFs are able to suppress the RGC fate by a similar mechanism as Ptf1a. Therefore, Foxn4 may directly and/or indirectly activate the expression of all 3 bHLH TF genes *Ptf1a*, *Neurod4*, and *Neurod1*, which in turn suppress the expression of *Atoh7* and *Pou4f2* involved in RGC competence and specification (Fig. 9*B*).

Despite the expected up-regulation of *Atoh7* expression in the absence of *Foxn4*, however, it is puzzling that we did not observe any obvious increase of *Atoh7* expression in E14.5 *Foxn4*$^{lacZ/lacZ}$ retinas (14), suggesting that *Atoh7* may be regulated also by other unknown mechanisms which might compromise the expected up-regulation. Inspection of the microarray data of P1 *Otx2* conditional knockout retinas (42) and RNA-seq data of P2 *Nrl*$^{-/-}$ retinas (51) revealed down-regulation of *Atoh7* expression in these 2 mutant retinas, suggesting that Otx2 and Nrl might be involved in activating *Atoh7* expression. If so, the significant down-regulation of Otx2 and Nrl expression would be able to compromise the expected up-regulation of *Atoh7* in *Foxn4*-null retinas. Interestingly, *Otx2* inactivation leads to up-regulation in the expression of Dlx1 and Dlx2 (42), which represent an alternative pathway for RGC generation (52).

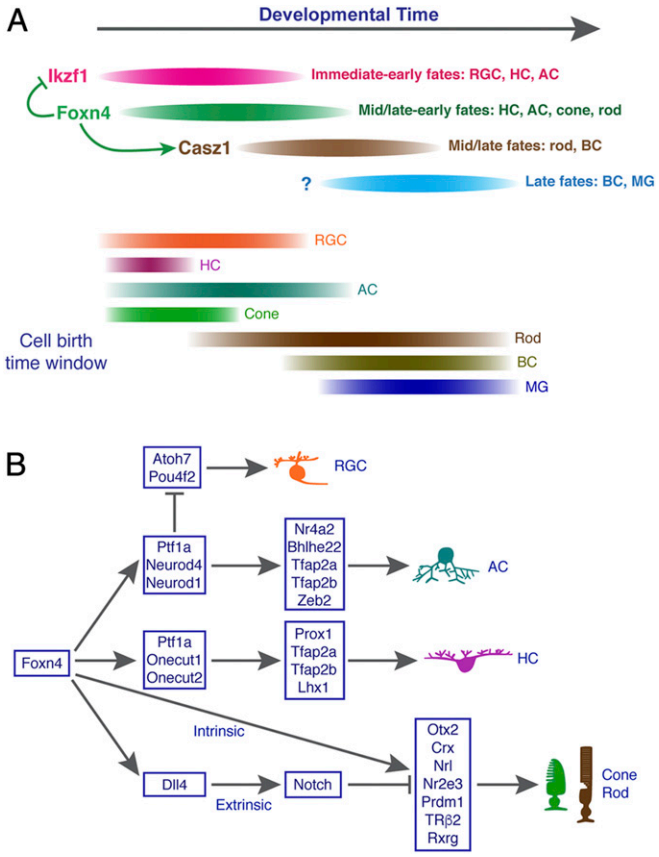

Fig. 9. Temporal patterning role of Foxn4 during retinogenesis. (*A*) Retinal cell types are born in a sequential yet overlapping manner. Foxn4 may confer early retinal progenitors with the competence to generate mid/late-early cell types including horizontal, amacrine, cone, and rod cells. It may facilitate transitions of RPC temporal identities by activating Casz1 expression but repressing Ikzf1 expression. (*B*) Foxn4 intrinsically confers retinal progenitors with the competence to generate cones and rods by activating the expression of Otx2, Crx, Nrl, Nr2e3, Prdm1, TRβ2, and Rxrg, which are required for photoreceptor fate determination and differentiation. It also directly activates Dll4-Notch signaling, which serves as an extrinsic signal to repress the expression of these photoreceptor TFs in neighboring cells. Foxn4 confers the progenitors with the competence of amacrine and horizontal cell generation by activating the expression of pertinent TFs including Ptf1a, Neurod4, Neurod1, Onecut1, and Onecut2, which are involved in the specification and differentiation of these 2 cell types. Meanwhile, Foxn4 inhibits RGC fate also by activating the expression of Ptf1a, Neurod4, and Neurod1, which have the activity to repress the expression of Atoh7 and Pou4f2. AC, amacrine cell; BC, bipolar cell; HC, horizontal cell; MG, Müller glia.

Foxn4 Is Indirectly Required for Retinal Synaptogenesis and Long-Term Maintenance. In this study, we investigated the functional requirement of Foxn4 in adult mouse retinas by generating a conditional *Foxn4* allele to circumvent the issue that conventional targeted *Foxn4* deletion causes a lethal phenotype during neonatal and early postnatal stages (14). These conditional knockout experiments revealed that retina-specific ablation of *Foxn4* results in disrupted OPL, down-regulation of synaptogenic marker expression, impaired formation of the triad synapses among photoreceptor, bipolar and horizontal cells, progressive retinal degeneration, and severely reduced ERG responses. A number of mutations disrupting the normal presynaptic triad development destroy the OPL morphology, typically with irregular and thinner OPL and bipolar neurites overextending into the outer nuclear layer, as seen in mutations of the L-VDCC subunit β2 (53), Cacna1f (54), calmodulin-like neuronal Ca^{2+}-binding protein CaBP4 (55), and ribbon-anchoring protein Bassoon (56), as well as of genes affecting horizontal cell development such as *Lhx1* (38) and *Onecut1* (37). These phenotypes were successfully duplicated in transgenic mice ectopically expressing the diphtheria toxin (DT) receptor which exclusively ablates horizontal cells upon DT administration (39). Given that *Foxn4* inactivation leads to complete failure of horizontal cell generation, the adult retinal phenotypes observed in $Foxn4^{\Delta fl/\Delta fl}$ mice most likely result from secondary effects of horizontal cell loss.

Physiologically, mature horizontal cells provide negative or sometimes positive feedback signals to photoreceptors. In the hallmark triad structure of the OPL, the synaptic ribbon of a rod or a cone and the lateral horizontal cells make up the presynaptic structure, modulating a spike signal before it is transmitted to 1 or 2 postsynaptic bipolar cells (57–60). Consistent with the morphological and structural abnormalities in the triad and OPL, mutations affecting presynaptic triads cause visual signal transmission defects from photoreceptors to bipolar cells. As reflected by ERG responses, the a wave is essentially normal in the beginning but the b wave is absent or seriously reduced (37–39, 53–56) (this study). This is also a phenotype found in human patients with congenital stationary night blindness (CSNB) (61, 62). The presynaptic (including the horizontal cell) mutations are usually associated with incomplete-type CSNB. In the long run, however, the a wave is slowly yet steadily reduced in scotopic ERG, accompanied by gradual thinning of the outer nuclear layer, due to photoreceptor degeneration in these mutants (37, 39, 63) (this study), a phenotype often missed by researchers. Whether this is a universal phenotype in presynaptic triad mutants remains to be investigated. The degeneration of photoreceptors was also found in human patients with presynaptic *CACNA1F* or *CACNA2D4* mutations (64, 65). The underlying mechanism leading to photoreceptor degeneration is still unclear, presumably due to loss of photoreceptor synapses, loss of lateral inhibition from horizontal cells, accumulation of neurotransmitter glutamate, perturbation of local metabolism causing oxidative stress, or a combination (39). Together, our current work and previous studies help to reveal an underappreciated role of horizontal cells in the establishment and maintenance of retinal laminar structure, synaptogenesis, visual signal transduction, and photoreceptor survival.

In summary, to further understand the retinal function of Foxn4 during development and in the adult, we performed a cluster analysis of Foxn4-dependent genes at different developmental stages, carried out RNA-seq analysis of *Foxn4*-null retinas, and generated a retina-specific conditional *Foxn4*-knockout allele. Combining functional data from the conventional and conditional knockout mouse lines rather than relying on a homolog screening approach, we found that Foxn4 most likely acts as a tTF during retinogenesis to bias RPCs toward the competence states of generating the mid/late-early cell types: cone, rod, amacrine, and horizontal cells, while suppressing the competence of generating the immediate-early cell type: RGCs. Additionally, because of its requirement for horizontal cell generation, Foxn4 may be indirectly involved in the synaptogenesis, visual signal transmission, and long-term survival of the retina.

Materials and Methods

A detailed description of experimental procedures and analyses is provided in *SI Appendix, Experimental Procedures*. Briefly, total RNA was isolated from retinas of wild-type and $Foxn4^{lacZ/lacZ}$ embryos for microarray and RNA-seq analyses. A floxed *Foxn4* allele was obtained by inserting loxP sites in introns 2 and 3 by homologous recombination in mouse ES cells. Alterations in gene and protein expression were investigated by qRT-PCR, RNA in situ hybridization, and immunostaining. All experiments on animals were performed according to institutional animal care and use committee standards, and approved by the Zhongshan Ophthalmic Center, Sun Yat-sen University, and Rutgers, the State University of New Jersey.

Data Availability. All data needed to evaluate the conclusions in this paper are present in the paper and/or *SI Appendix*. Additional data related to this paper may be requested from the authors.

ACKNOWLEDGMENTS. We thank Drs. Dongchang Xiao and Zuming Zhang for thoughtful comments on the manuscript. This work was supported in part by the National Natural Science Foundation of China (Grants 81670862, 81721003, 31871497, 81870682), National Key R&D Program of China (Grant 2017YFA0104100), National Basic Research Program (973 Program) of China (Grant 2015CB964600), Local Innovative and Research Teams Project of Guangdong Pearl River Talents Program, Science and Technology Planning Projects of Guangzhou City (Grants 201904020036, 201904010358), and Fundamental Research Funds of the State Key Laboratory of Ophthalmology, Sun Yat-sen University.

1. R. W. Young, Cell differentiation in the retina of the mouse. *Anat. Rec.* **212**, 199–205 (1985).
2. D. H. Rapaport, L. L. Wong, E. D. Wood, D. Yasumura, M. M. LaVail, Timing and topography of cell genesis in the rat retina. *J. Comp. Neurol.* **474**, 304–324 (2004).
3. R. L. Sidman, "Histogenesis of mouse retina studied with thymidine-^{3}H" in *The Structure of the Eye*, G. Smelser, Ed. (Academic Press, New York, 1961), pp. 487–506.
4. C. L. Cepko, The roles of intrinsic and extrinsic cues and bHLH genes in the determination of retinal cell fates. *Curr. Opin. Neurobiol.* **9**, 37–46 (1999).
5. F. J. Livesey, C. L. Cepko, Vertebrate neural cell-fate determination: Lessons from the retina. *Nat. Rev. Neurosci.* **2**, 109–118 (2001).
6. W. A. Harris, Cellular diversification in the vertebrate retina. *Curr. Opin. Genet. Dev.* **7**, 651–658 (1997).
7. M. Xiang, Intrinsic control of mammalian retinogenesis. *Cell. Mol. Life Sci.* **70**, 2519–2532 (2013).
8. N. Konstantinides, A. M. Rossi, C. Desplan, Common temporal identity factors regulate neuronal diversity in fly ventral nerve cord and mouse retina. *Neuron* **85**, 447–449 (2015).
9. C. Q. Doe, Temporal patterning in the *Drosophila* CNS. *Annu. Rev. Cell Dev. Biol.* **33**, 219–240 (2017).
10. X. Li, Z. Chen, C. Desplan, Temporal patterning of neural progenitors in *Drosophila*. *Curr. Top. Dev. Biol.* **105**, 69–96 (2013).
11. B. J. Pearson, C. Q. Doe, Regulation of neuroblast competence in *Drosophila*. *Nature* **425**, 624–628 (2003).
12. J. Elliott, C. Jolicoeur, V. Ramamurthy, M. Cayouette, Ikaros confers early temporal competence to mouse retinal progenitor cells. *Neuron* **60**, 26–39 (2008).
13. P. Mattar, J. Ericson, S. Blackshaw, M. Cayouette, A conserved regulatory logic controls temporal identity in mouse neural progenitors. *Neuron* **85**, 497–504 (2015).
14. S. Li *et al*., Foxn4 controls the genesis of amacrine and horizontal cells by retinal progenitors. *Neuron* **43**, 795–807 (2004).
15. N. J. Kunzevitzky *et al*., Foxn4 is required for retinal ganglion cell distal axon patterning. *Mol. Cell. Neurosci.* **46**, 731–741 (2011).
16. H. Boije, P. H. Edqvist, F. Hallböök, Temporal and spatial expression of transcription factors FoxN4, Ptf1a, Prox1, Isl1 and Lim1 mRNA in the developing chick retina. *Gene Expr. Patterns* **8**, 117–123 (2008).
17. H. Luo *et al*., Forkhead box N4 (Foxn4) activates Dll4-Notch signaling to suppress photoreceptor cell fates of early retinal progenitors. *Proc. Natl. Acad. Sci. U.S.A.* **109**, E553–E562 (2012).
18. H. Boije, S. Shirazi Fard, H. Ring, F. Hallböök, Forkheadbox N4 (FoxN4) triggers context-dependent differentiation in the developing chick retina and neural tube. *Differentiation* **85**, 11–19 (2013).
19. M. M. Islam, Y. Li, H. Luo, M. Xiang, L. Cai, Meis1 regulates Foxn4 expression during retinal progenitor cell differentiation. *Biol. Open* **2**, 1125–1136 (2013).
20. S. Li, K. Misra, M. P. Matise, M. Xiang, Foxn4 acts synergistically with Mash1 to specify subtype identity of V2 interneurons in the spinal cord. *Proc. Natl. Acad. Sci. U.S.A.* **102**, 10688–10693 (2005).
21. S. Li, K. Misra, M. Xiang, A Cre transgenic line for studying V2 neuronal lineages and functions in the spinal cord. *Genesis* **48**, 667–672 (2010).
22. K. Misra, H. Luo, S. Li, M. Matise, M. Xiang, Asymmetric activation of Dll4-Notch signaling by Foxn4 and proneural factors activates BMP/TGFβ signaling to specify V2b interneurons in the spinal cord. *Development* **141**, 187–198 (2014).
23. M. Xiang, S. Li, Foxn4: A multi-faceted transcriptional regulator of cell fates in vertebrate development. *Sci. China Life Sci.* **56**, 985–993 (2013).
24. S. Li, M. Xiang, Foxn4 influences alveologenesis during lung development. *Dev. Dyn.* **240**, 1512–1517 (2011).
25. N. C. Chi *et al*., Foxn4 directly regulates tbx2b expression and atrioventricular canal formation. *Genes Dev.* **22**, 734–739 (2008).
26. E. P. Campbell, I. K. Quigley, C. Kintner, Foxn4 promotes gene expression required for the formation of multiple motile cilia. *Development* **143**, 4654–4664 (2016).
27. H. Liu *et al*., An isoform of retinoid-related orphan receptor β directs differentiation of retinal amacrine and horizontal interneurons. *Nat. Commun.* **4**, 1813 (2013).
28. Y. Fujitani *et al*., Ptf1a determines horizontal and amacrine cell fates during mouse retinal development. *Development* **133**, 4439–4450 (2006).
29. K. Jin, M. Xiang, Transcription factor Ptf1a in development, diseases and reprogramming. *Cell. Mol. Life Sci.* **76**, 921–940 (2019).
30. C. Li, W. H. Wong, "DNA-chip analyzer (dChip)" in *The Analysis of Gene Expression Data: Methods and Software*, G. Parmigiani, E. S. Garrett, R. Irizarry, S. L. Zeger, Eds. (Springer-Verlag, New York, 2003), pp. 120–141.
31. A. Sturn, J. Quackenbush, Z. Trajanoski, Genesis: Cluster analysis of microarray data. *Bioinformatics* **18**, 207–208 (2002).
32. A. Swaroop, D. Kim, D. Forrest, Transcriptional regulation of photoreceptor development and homeostasis in the mammalian retina. *Nat. Rev. Neurosci.* **11**, 563–576 (2010).
33. B. S. Clark *et al*., Single-cell RNA-seq analysis of retinal development identifies NFI factors as regulating mitotic exit and late-born cell specification. *Neuron* **102**, 1111–1126.e5 (2019).
34. K. Jin *et al*., Tfap2a and 2b act downstream of Ptf1a to promote amacrine cell differentiation during retinogenesis. *Mol. Brain* **8**, 28 (2015).
35. F. W. Farley, P. Soriano, L. S. Steffen, S. M. Dymecki, Widespread recombinase expression using FLPeR (flipper) mice. *Genesis* **28**, 106–110 (2000).
36. Y. Furuta, O. Lagutin, B. L. Hogan, G. C. Oliver, Retina- and ventral forebrain-specific Cre recombinase activity in transgenic mice. *Genesis* **26**, 130–132 (2000).
37. F. Wu *et al*., Onecut1 is essential for horizontal cell genesis and retinal integrity. *J. Neurosci.* **33**, 13053–13065 (2013).
38. P. W. Keeley *et al*., Development and plasticity of outer retinal circuitry following genetic removal of horizontal cells. *J. Neurosci.* **33**, 17847–17862 (2013).
39. S. Sonntag *et al*., Ablation of retinal horizontal cells from adult mice leads to rod degeneration and remodeling in the outer retina. *J. Neurosci.* **32**, 10713–10724 (2012).
40. C. L. Cepko, The determination of rod and cone photoreceptor fate. *Annu. Rev. Vis. Sci.* **1**, 211–234 (2015).
41. X. Li *et al*., Temporal patterning of *Drosophila* medulla neuroblasts controls neural fates. *Nature* **498**, 456–462 (2013).
42. Y. Omori *et al*., Analysis of transcriptional regulatory pathways of photoreceptor genes by expression profiling of the Otx2-deficient retina. *PLoS One* **6**, e19685 (2011).
43. L. Gan *et al*., POU domain factor Brn-3b is required for the development of a large set of retinal ganglion cells. *Proc. Natl. Acad. Sci. U.S.A.* **93**, 3920–3925 (1996).
44. S. W. Wang *et al*., Requirement for math5 in the development of retinal ganglion cells. *Genes Dev.* **15**, 24–29 (2001).
45. N. L. Brown, S. Patel, J. Brzezinski, T. Glaser, Math5 is required for retinal ganglion cell and optic nerve formation. *Development* **128**, 2497–2508 (2001).
46. F. Qiu, H. Jiang, M. Xiang, A comprehensive negative regulatory program controlled by Brn3b to ensure ganglion cell specification from multipotential retinal precursors. *J. Neurosci.* **28**, 3392–3403 (2008).
47. T. C. Badea, H. Cahill, J. Ecker, S. Hattar, J. Nathans, Distinct roles of transcription factors brn3a and brn3b in controlling the development, morphology, and function of retinal ganglion cells. *Neuron* **61**, 852–864 (2009).
48. M. Xiang *et al*., Brn-3b: A POU domain gene expressed in a subset of retinal ganglion cells. *Neuron* **11**, 689–701 (1993).
49. H. Nakhai *et al*., Ptf1a is essential for the differentiation of GABAergic and glycinergic amacrine cells and horizontal cells in the mouse retina. *Development* **134**, 1151–1160 (2007).
50. T. Inoue *et al*., Math3 and NeuroD regulate amacrine cell fate specification in the retina. *Development* **129**, 831–842 (2002).
51. J. W. Kim *et al*., NRL-regulated transcriptome dynamics of developing rod photoreceptors. *Cell Rep.* **17**, 2460–2473 (2016).
52. J. de Melo *et al*., Dlx1 and Dlx2 function is necessary for terminal differentiation and survival of late-born retinal ganglion cells in the developing mouse retina. *Development* **132**, 311–322 (2005).
53. S. L. Ball *et al*., Role of the β(2) subunit of voltage-dependent calcium channels in the retinal outer plexiform layer. *Invest. Ophthalmol. Vis. Sci.* **43**, 1595–1603 (2002).
54. F. Mansergh *et al*., Mutation of the calcium channel gene Cacna1f disrupts calcium signaling, synaptic transmission and cellular organization in mouse retina. *Hum. Mol. Genet.* **14**, 3035–3046 (2005).
55. F. Haeseleer *et al*., Essential role of Ca^{2+}-binding protein 4, a Cav1.4 channel regulator, in photoreceptor synaptic function. *Nat. Neurosci.* **7**, 1079–1087 (2004).
56. O. Dick *et al*., The presynaptic active zone protein Bassoon is essential for photoreceptor ribbon synapse formation in the retina. *Neuron* **37**, 775–786 (2003).
57. T. Baden, T. Euler, M. Weckström, L. Lagnado, Spikes and ribbon synapses in early vision. *Trends Neurosci.* **36**, 480–488 (2013).
58. S. tom Dieck, J. H. Brandstätter, Ribbon synapses of the retina. *Cell Tissue Res.* **326**, 339–346 (2006).
59. W. B. Thoreson, S. C. Mangel, Lateral interactions in the outer retina. *Prog. Retin. Eye Res.* **31**, 407–441 (2012).
60. P. Sterling, G. Matthews, Structure and function of ribbon synapses. *Trends Neurosci.* **28**, 20–29 (2005).
61. M. A. McCall, R. G. Gregg, Comparisons of structural and functional abnormalities in mouse b-wave mutants. *J. Physiol.* **586**, 4385–4392 (2008).
62. Y. Miyake, K. Yagasaki, M. Horiguchi, Y. Kawase, T. Kanda, Congenital stationary night blindness with negative electroretinogram. A new classification. *Arch. Ophthalmol.* **104**, 1013–1020 (1986).
63. K. A. Wycisk *et al*., Structural and functional abnormalities of retinal ribbon synapses due to Cacna2d4 mutation. *Invest. Ophthalmol. Vis. Sci.* **47**, 3523–3530 (2006).
64. N. T. Bech-Hansen *et al*., Loss-of-function mutations in a calcium-channel alpha1-subunit gene in Xp11.23 cause incomplete X-linked congenital stationary night blindness. *Nat. Genet.* **19**, 264–267 (1998).
65. K. A. Wycisk *et al*., Mutation in the auxiliary calcium-channel subunit CACNA2D4 causes autosomal recessive cone dystrophy. *Am. J. Hum. Genet.* **79**, 973–977 (2006).